INFECTION AND IMMUNITY, Feb. 2003, p. 891–903 Vol. 71, No. 2
0019-9567/03/$08.00+0 DOI: 10.1128/IAI.71.2.891–903.2003

Phagocytosis and Intracellular Fate of *Aspergillus fumigatus* Conidia in Alveolar Macrophages

O. Ibrahim-Granet,[1]* B. Philippe,[1] H. Boleti,[2]† E. Boisvieux-Ulrich,[3] D. Grenet,[4] M. Stern,[4] and J. P. Latgé[1]*

Unité des Aspergillus, Institut Pasteur,[1] and Unité de Biologie des Interactions Cellulaires, Institut Pasteur, CNRS URA 1960,[2] 75724 Paris Cedex 15, Laboratoire de Cytophysiologie et Toxicologie Cellulaire, Université Paris VII, Paris,[3] and Service de Pneumologie, Hôpital Foch, 92 151 Suresnes Cedex,[4] France

Received 5 July 2002/Returned for modification 15 August 2002/Accepted 13 November 2002

***Aspergillus fumigatus* is the most prevalent airborne fungal pathogen responsible for fatal invasive aspergillosis in immunocompromised patients. Upon arrival in the lung alveolus, conidia of *A. fumigatus* are phagocytosed by alveolar macrophages, the major phagocytic cells of the lung. Engulfment and intracellular trafficking of *A. fumigatus* conidia in alveolar macrophages of two different origins, the murine cell line MH-S and human pulmonary alveolar macrophages, were analyzed by electron microscopy and immunofluorescence. Phagocytosis of *A. fumigatus* conidia required actin polymerization and phosphatidylinositol 3-kinase activity. Fusion of *A. fumigatus* phagosomes with early and late endosomes was shown by immunolabeling with specific markers for the transferrin receptor, early endosome antigen, and Rab7. Maturation of *A. fumigatus* phagolysosomes was monitored by using a fixable acidotropic probe, LysoTracker Red DND-99, and an anti-cathepsin D antibody. Bafilomycin A-induced inhibition of lysosomal acidification abolished the conidial killing by the macrophages. These data suggest that the maturation of *A. fumigatus* phagosomes results from fusion with the compartments of the endocytic pathway and that the killing of conidia depends on phagolysosome acidification. A model for the phagocytosis of *A. fumigatus* conidia by alveolar macrophages is proposed on the basis of these results.**

Professional phagocytes have as a primary function the engulfment of microbial invaders within a membrane-bound compartment called a phagosome. This phagocytic activity requires the assembly of actin filaments from actin monomers and oligomers localized underneath the plasma membrane at sites where contact is made with the phagocytosed particle (2, 35, 36, 42). The maturation of phagosomes into lysosomes is normally a complex process involving membrane budding and fusion events with different compartments of the endocytic pathway and recruitment of various factors like small GTPases of the Rab family, hydrolytic enzymes, and proton pumps (5, 7, 11, 32, 45).

Most phagocytosed microorganisms are killed in the lysosome. However, some pathogens are known to block or alter the traffic and/or maturation of the membrane-bound compartments in which they reside within the host cells (6, 30, 63, 64) and thereby evade destruction by the lysosomal hydrolases.

Aspergillus fumigatus is a common fungal member of the airborne microbial population that is present both indoors and outdoors (46). Conidia of this fungal species are continuously inhaled by humans and reach all levels of the respiratory tract. In immunocompetent patients, the major phagocytic cells of the lung, alveolar macrophages (AMs), kill the conidia of *A. fumigatus* as well as any other inhaled microbial invader. In immunocompromised patients, especially those who have undergone bone marrow or solid-organ transplantation, conidia often germinate and the mycelium invades the lung parenchyma. Invasive pulmonary aspergillosis, a result of this mycelial development, is a lethal disease for most immunocompromised patients infected with *A. fumigatus*.

Little is known about the cellular mechanisms of internalization and killing of *A. fumigatus* by AMs in immunocompetent patients. Such knowledge is an essential requirement for understanding the mechanisms which allow conidia to escape death under immunosuppressive treatments.

In this study, we investigated the engulfment and intracellular trafficking of *A. fumigatus* conidia by AMs of two different origins, the murine cell line MH-S and primary cultures of human pulmonary AMs. Our study showed that the two cell types have similar mechanisms for phagocytosis of conidia: (i) actin polymerization and phosphatidylinositol (PI) 3-kinase activity are required for the initial steps of phagocytosis, and (ii) maturation of the *A. fumigatus* phagosome yields a phagolysosome, with conidial killing being dependent on the acidification of this compartment.

MATERIALS AND METHODS

Antibodies and chemical reagents. The following primary antibodies were used in this study: a rabbit polyclonal antibody (pAb) specific for *A. fumigatus* conidia (67), two anti-transferrin receptor (anti-TfR) monoclonal antibodies (MAbs) (RI7-217 and OKT9; American Type Culture Collection) recognizing the murine or human TfR (kindly provided by A. Dautry, Institut Pasteur), a mouse anti-early endosomal antigen 1 (anti-EEA1; Transduction Laboratories) MAb recognizing the human protein, an anti-Rab7 pAb (52) (kindly provided by S. Méresse, CIML, Marseille, France), two anti-LAMP1 MAbs recognizing the

* Corresponding author. Mailing address for O. Ibrahim-Granet: Unité des Aspergillus, Institut Pasteur, 25 rue du Dr. Roux, 75724 Paris Cedex 15, France. Phone: 33 0 1 40 61 35 18. Fax: 33 0 1 40 61 34 19. E-mail: ogranet@pasteur.fr. E-mail address for J. P. Latgé: jplatge@pasteur.fr.

† Present address: Molecular Virology Laboratory, Hellenic Pasteur Institute, Athens 11521, Greece.

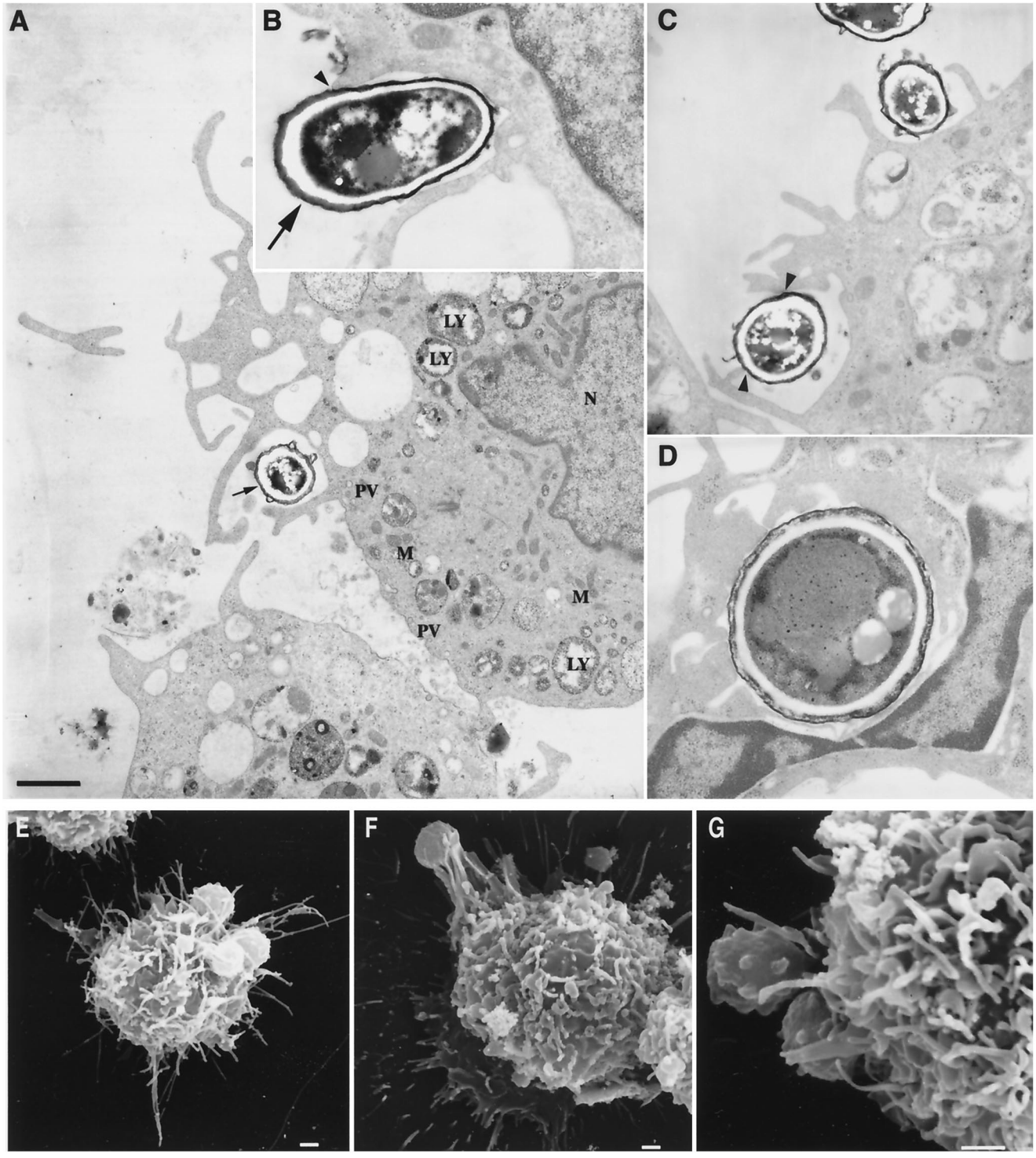

FIG. 1. Internalization of conidia by HAMs, as revealed by transmission electron microscopy (A to D), and MH-S cells, as revealed by scanning electron microscopy (E to G). Panels A to C show the early stages of engulfment after 5 min of contact between conidia and HAMs. Note the numerous lysosomes (LY) widely distributed throughout the cell. PV, pinocytic vesicles; M, mitochondria; N, nuclei. Also, note the double-layered cell wall (arrows) with the electron-dense pigmented outer layer of the conidium in panels A and B, the contact points (arrowheads) between conidia and AM pseudopodia in panels B and C, and the progressive engulfment of the conidium by AM pseudopodia. Panel D shows the late stage of engulfment after 90 min. Panels E to G show conidia bound to a macrophage analyzed 5 min after the beginning of ingestion. Note the extensions of pseudopodia towards the conidium and the contact of these pseudopodia with the conidial cell wall in panels F and G. Bars, 2 μm (A) and 1 μm (E to G).

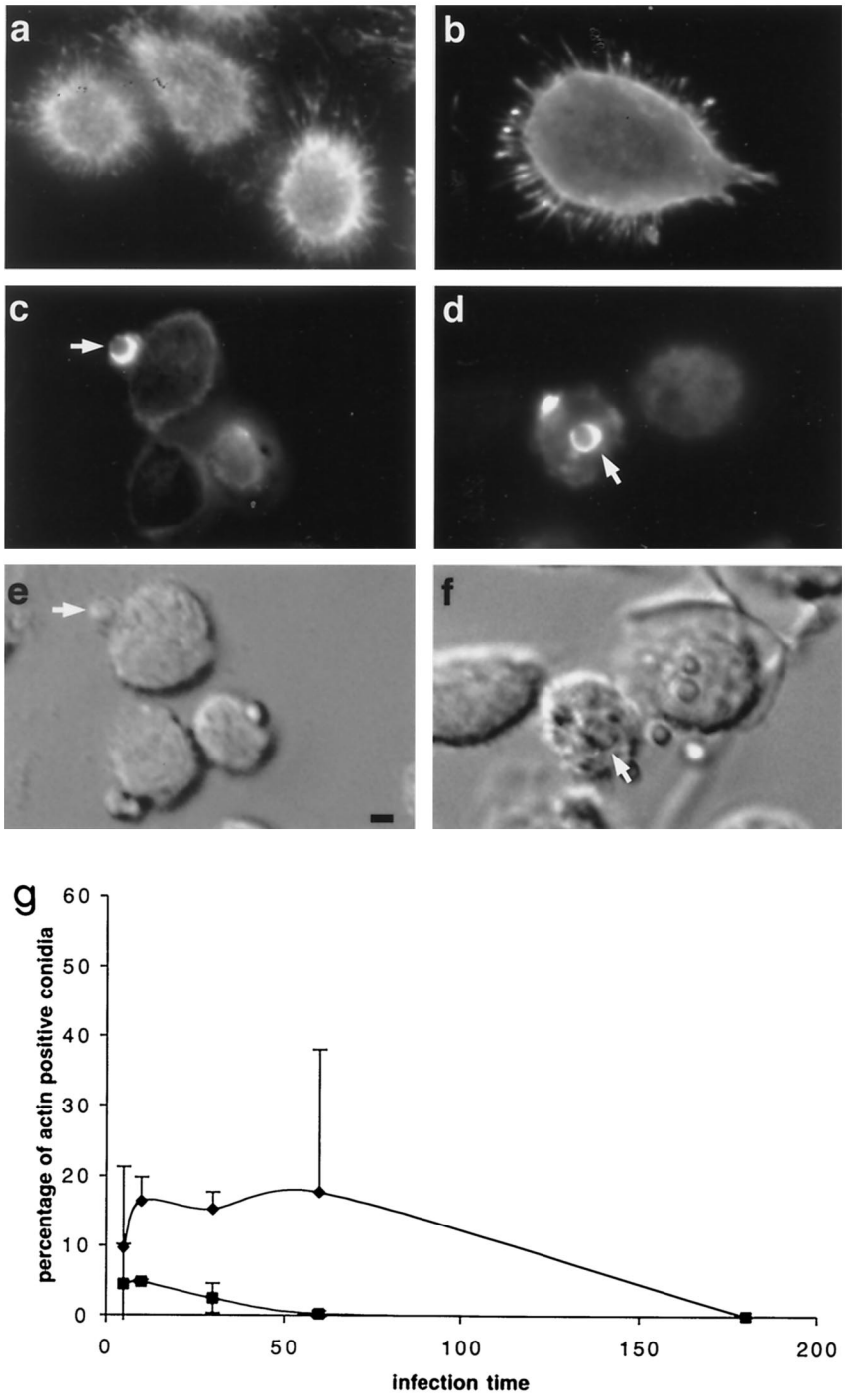

FIG. 2. F-actin staining, with Texas Red-phalloidin, of MH-S cells (a, c, and e) and HAMs (b, d, and f) during the engulfment of conidia. Panels a and b show control cells. Note the phagocytic cup in panel c and the actin ring surrounding an ingested conidium in panel d (arrows). Panels e and f contain differential interference contrast (DIC) images of what is shown in panels c and d, respectively. Bar, 2 μm. (g) Kinetics of actin involvement in conidia phagocytosis. The percentage of actin-positive conidia was calculated as follows: (the number of conidia surrounded by an actin ring or cup stained with Texas Red-phalloidin/the total number of conidia associated to macrophages × 100. Data are averages from three independent experiments, and standard deviations are indicated with error bars. ♦, HAMs; ■, MH-S cells. Infection times are in minutes.

human and the murine proteins (CD107a; PharMingen), and an anti-human cathepsin D pAb (43) (kindly provided by W. Gregory, Washington University School of Medicine). Purified rabbit immunoglobulin G (IgG; Sigma), mouse IgG1, and rat IgG2a isotypes (PharMingen) were used as primary control antibodies.

A Texas Red-conjugated goat anti-rabbit IgG, a fluorescein 5-isothiocyanate (FITC)-conjugated goat anti-rabbit IgG, and a Texas Red-conjugated goat anti-mouse IgG (Jackson Immunoresearch Laboratories) were used as secondary antibodies. The acidotropic dye LysoTracker Red DND-99, Texas Red-phalloidin, and Höechst 33342 dye were purchased from Molecular Probes (Eugene,

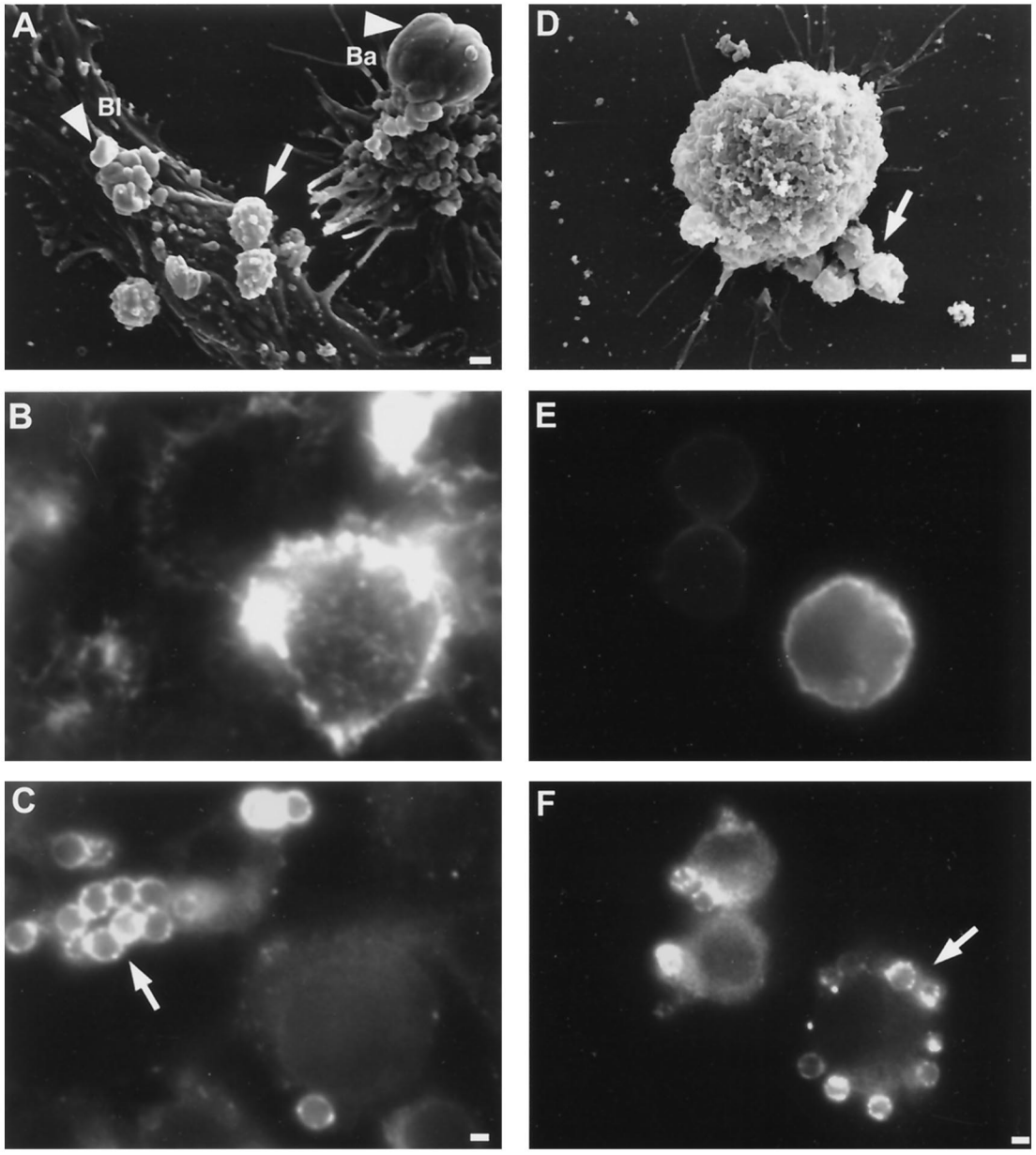

FIG. 3. Effect of cytochalasin D and wortmannin treatment on MH-S cells. MH-S cells were treated for 30 min with 2 μM cytochalasin D (A to C) or 1 μM wortmannin (D to F), and ingestion of conidia was performed in the presence of the drug. Shown are scanning electron micrographs of cells at 5 (A) and 30 (D) min postingestion. Arrowheads in panel A indicate blebs (Bl) and balloons (Ba), which are probably nuclei on the top of treated cells. The arrows in panels A and D indicate uningested conidia. Also shown are cells at 60 min postingestion (B, C, E, and F). Cells were fixed, treated with anti-conidia antibody, stained with an FITC-conjugated antibody to label uningested conidia (C and F), permeabilized, and incubated with Texas Red-phalloidin to label actin (B and E). Note the brightly stained aggregates of actin and the lack of F-actin rich filopodia in panels B and E; nonphagocytosed conidia (arrows) can be seen on the surface of MH-S cells in panels C and F. Bars, 1 μm.

Oreg.). Cytochalasin D, wortmannin, and bafilomycin A were purchased from Sigma.

Fungal strains. *A. fumigatus* strain CBS 144.89 was a clinical isolate. Conidia were harvested by washing a 7-day-old slant culture with phosphate-buffered saline (PBS) supplemented with 0.1% Tween 20. The suspension was filtered through a 40-μm-pore-size cell strainer (Falcon) to separate conidia from contaminating mycelium. In the killing experiments, the conidia were labeled with FITC as previously described (67). Briefly, freshly harvested conidia (2×10^7/10 ml of 0.05 M Na carbonate buffer [pH 10.2]) were incubated with FITC at a final concentration of 0.1 mg/ml at 37°C for 1 h and washed by centrifugation three times in PBS–0.1% Tween 20.

Cells. Human AMs (HAMs) were obtained from bronchoalveolar lavage (BAL) of 11 patients who had received lung transplants in the Hôpital Foch (Suresne, France) between 1997 and 2000. All patients were initially maintained on an immunosuppressive regimen of prednisone, cyclosporine, and azathioprine. FK506 was substituted for cyclosporine after three consecutive acute lung rejections (16). The lung transplantation protocol was approved by the Hôpital Foch institutional review board for human studies, and informed consent was

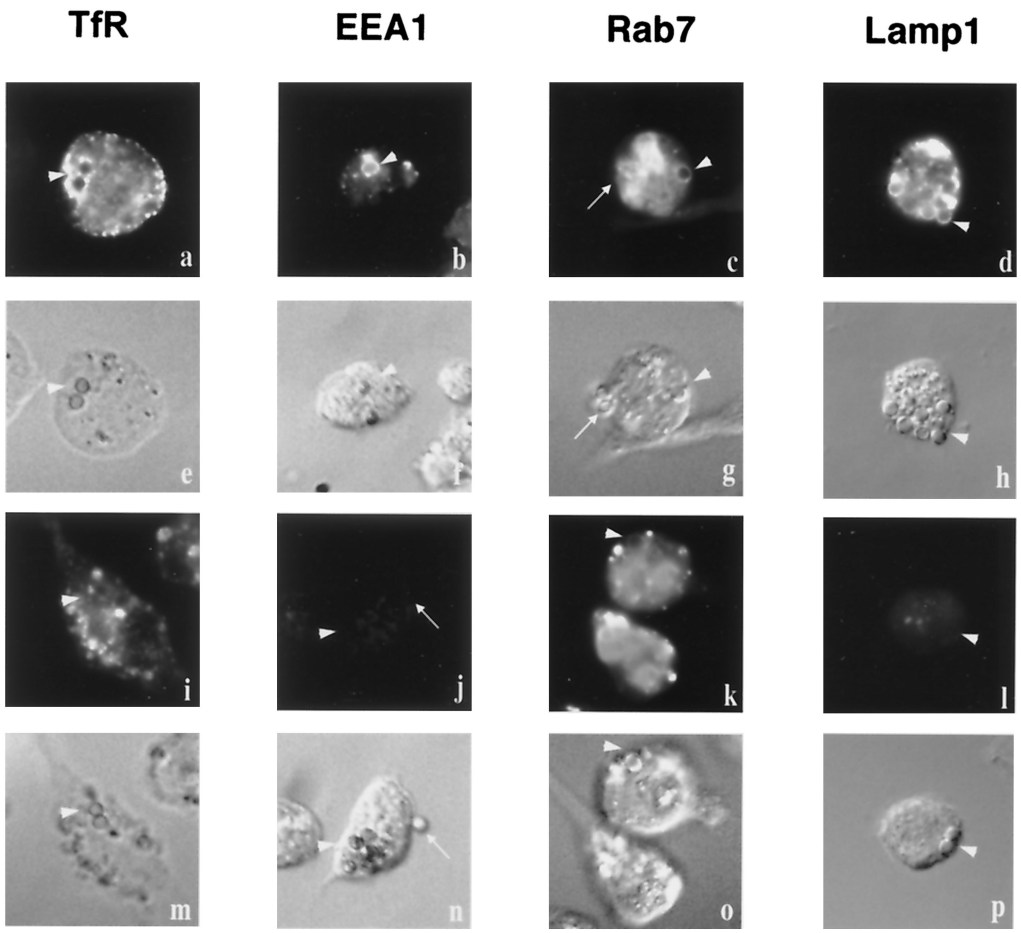

FIG. 4. Maturation of *A. fumigatus*-containing phagosomes in HAMs. HAMs were incubated with conidia (2:1 ratio of conidia to macrophages) and were fixed at 5, 10, 30, and 60 min after the beginning of phagocytosis. After permeabilization with saponin, cells were labeled at 10 min (a to c and e to g) or 60 min (d and h to p) postingestion with the specific monoclonal or polyclonal anti-TfR (1/1,000), anti-EEA1 (1/500), anti-Rab 7 (1/50), and anti-Lamp1 (1/100) antibodies and secondary antibodies conjugated to Texas Red. (a to c) Arrowheads indicate TfR-positive (a), EEA1-positive (b), and Rab 7-positive (c) staining surrounding the conidia. (d) Cells were labeled at 60 min postingestion, and the arrowhead indicates positive staining for Lamp1. (e to h) Corresponding DIC images. The arrowheads indicate conidia. Note that the conidia outside the cells (thin arrows in panels c, g, j, and n) were not labeled by the same antibodies. (i to k) Lack of labeling with the anti-TfR, anti-EEA1, and anti-Rab7 antibodies. (l) Cells were labeled with control IgG1 MAb. (m to p) Corresponding DIC images. Bar, 2 μm.

obtained from each individual after a detailed description of the procedure was provided. According to French legislation, since the cells used did not result from a supplementary surgical operation done for the purpose of the study, the approval of the Comité Consultatif de Protection des Personnes dans la Recherche Biomédicale was not required.

BALs were performed regularly following transplantation once a month during the first 6 months and once every 6 months thereafter to detect asymptomatic posttransplantation complications or for diagnosis of other complications suspected on clinical and/or functional grounds (16).

Cells from BAL were harvested by centrifugation (400 × *g* for 8 min at 4°C), and the cell pellet was resuspended in RPMI complete medium containing 10% fetal bovine serum and plated on 12-mm-diameter glass coverslips at a density of 3×10^5 to 5×10^5 cells per coverslip. Nonadherent cells were removed by washing after a 2-h incubation at 37°C in an atmosphere of 5% CO_2. Viability was always more than 95% by the dye exclusion test with trypan blue.

MH-S murine AMs (49), derived by simian virus 40 transformation of mouse AMs, were cultured in RPMI complete medium containing 10% fetal bovine serum and maintained in an incubator at 37°C in an atmosphere of 5% CO_2. MH-S cells were plated 24 h prior to experimentation.

Phagocytosis assay. AMs were challenged with two conidia per macrophage and were subsequently incubated at 4°C for 30 min. Unbound conidia were removed by washing with cold RPMI complete medium, and phagocytosis of the bound conidia was initiated by shifting the cells to 37°C in an atmosphere of 5% CO_2.

At the end of each incubation period, phagocytosis was stopped by washing the AMs with ice-cold PBS and subjecting them to fixation with 3% paraformaldehyde in PBS (10 min at room temperature [RT]) followed by three washes with 50 mM NH_4Cl in PBS. To avoid nonspecific binding of antibodies, cells were subsequently incubated (30 min at RT) in a blocking solution consisting of 5% goat serum and 5% human serum in PBS (for HAMs) or 5% goat serum and 5% mouse serum in PBS (for MH-S cells).

The number of *A. fumigatus* conidia engulfed by macrophages was determined by immunofluorescence using the anti-conidia antibody and a secondary antibody conjugated to Texas Red as previously described (67). For specific labeling of uningested conidia, AMs were incubated (30 min at RT) with a rabbit anti-conidia antiserum at a dilution of 1:50, washed three times with blocking solution, and finally incubated (30 min at RT) with the Texas Red-conjugated anti-rabbit antibody at a dilution of 1:200. Both antibodies were diluted in the corresponding blocking solution. The above-mentioned procedure allowed labeling of the uningested conidia only. The percentage of ingestion was estimated as the ratio of the number of ingested conidia to the total number of conidia bound to 100 AMs.

Assay for conidial killing. To quantify the killing of conidia following each infection period (4 or 18 h), the AMs were lysed by a water osmotic shock and

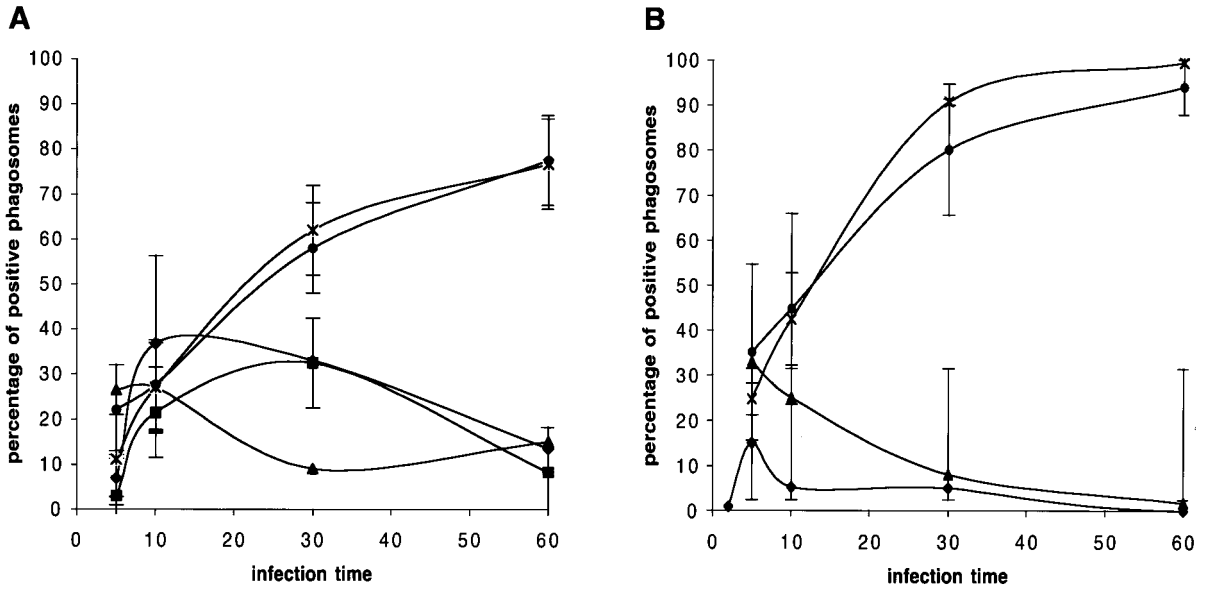

FIG. 5. Kinetics of maturation of *A. fumigatus*-containing phagosomes in AMs. Shown is the quantification of the immunolabeling of conidia ingested by HAMs (A) and MH-S cells (B) with antibodies directed against various endocytic markers as described in the legend to Fig. 4. The percentages shown are the number of phagosomes labeled with the antibody divided by the total number of phagosomes containing conidia. Data are means from three independent experiments, and standard deviations are indicated with error bars. Infection times are in minutes. ●, percentage of ingestion; ✕, percentage of Lamp1-positive phagosomes; ♦, percentage of TrfR-positive phagosomes; ▲, percentage of Rab7-positive phagosomes; ■, percentage of EEA1-positive phagosomes.

homogenate containing conidia was then incubated in an equal volume of 2× Sabouraud (4% glucose–2% mycopeptone) culture medium at 37°C for 7 h. The percentage of killing was determined as follows: (the number of nongerminated conidia/the total number of conidia phagocytosed by the macrophages) × 100. Germination was counted under a light fluorescence microscope.

Immunofluorescence microscopy. For immunolocalization of markers of endocytic compartments, cells were fixed and blocked as described above and were permeabilized (30 min at RT) in blocking solution supplemented with 0.05% (wt/vol) saponin. Cells were then incubated (30 min at RT) with the primary antibodies diluted in blocking solution containing 0.05% saponin, washed three times with the same solution, and incubated (30 min at RT) with fluorochrome-conjugated (FITC or Texas Red) secondary antibodies. Purified rabbit IgG or monoclonal immunoglobulin isotypes were used for controls. For visualization of actin filaments, AMs were fixed as described above, permeabilized for 5 min with 0.1% Triton X-100 in PBS, and stained (30 min at RT) with Texas Red-labeled phalloidin.

Nuclei were labeled with Höechst 33342 dye (10 μg/ml;10 min at RT) diluted in blocking solution plus saponin. Coverslips were washed three times in PBS, mounted with Mowiol (62) sealed on microscope slides with nail polish, and stored at 4°C until observation. Samples were examined with a Zeiss Axiophot microscope attached to a cooled charge-coupled device camera (Photometrics). Images were obtained with the IPLab spectrum program (Signal Analytics, Vienna, Va.) and further processed with Adobe Photoshop software.

Treatment with drugs. To assess the roles of actin polymerization and the PI 3-kinase in the initial steps of phagocytosis of *A. fumigatus*, cells were pretreated (30 min at 37°C) prior to phagocytosis with either 2 to 4 μM cytochalasin D (22) or 0.1 to 1.0 μM wortmannin, a PI 3-kinase inhibitor (9).

Inhibition of the vacuolar ATPase (15) was done by preloading the cells 30 min before infection with 0.1 to 0.25 μM bafilomycin A. Infection was performed in the presence of bafilomycin A for up to 18 h. Concentrations of bafilomycin A up to 250 nM did not affect the viability of macrophages or the germination of *A. fumigatus* conidia.

Monitoring of phagosomal pH. Acidification of the phagosome was assessed by use of the acidotropic dye LysoTracker Red DND-99. Cells were preloaded with LysoTracker (diluted 1:20,000 [vol/vol] in RPMI complete medium) for 2 h and were subsequently infected at 4°C with *A. fumigatus* conidia in fresh medium without LysoTracker. After removal of uningested conidia, culture medium with LysoTracker was readded to each well and conidia internalization was initiated at 37°C. Infection was stopped after 1, 4, and 18 h, and the cells were washed with PBS, mounted on microscope slides, and examined immediately under the fluorescence microscope. Acidification control experiments were performed with uninfected cells or cells infected in the presence of 250 nM bafilomycin A.

Scanning electron microscopy. AMs were fixed (1 h at RT) with 2.5% glutaraldehyde in EM buffer (0.1 M Na cacodylate [pH 7.2]), washed with EM buffer, and then postfixed (1 h at RT) with 1% OsO_4 in 0.1 M Na cacodylate buffer. After being washed in EM buffer, the cells were dehydrated by serial treatment with 70 and 100% ethanol and acetone. Dehydration was then completed with acetone treatment. The coverslips were critical point dried, mounted onto scanning stubs, and air-dried overnight. Cells were sputter coated with 30 nM gold-palladium and examined on a Jeol JSM-6300F scanning electron microscope.

Transmission electron microscopy. AMs were fixed overnight at 4°C with 2.5% glutaraldehyde in EM buffer and washed in EM buffer. Postfixation (30 min) in aqueous 1% osmium tetroxide (OsO_4) in 0.1 M cacodylate buffer was followed by several washes (5 min each) in sodium acetate buffer (50 mM; pH 5; 0 to 2°C). Dehydration in an ethanol gradient preceded infiltration in Epon resin. Ultrathin (50 to 60 nM) sections were cut and stained with 5% uranyl acetate followed by lead citrate. The sections were examined using a Jeol GEM-1010 transmission electron microscope.

RESULTS

Phagocytosis of conidia by AMs. Internalization of *A. fumigatus* conidia by AMs was initially monitored by transmission and scanning electron microscopy (Fig. 1). Contact between AMs and conidia resulted in the formation of pseudopodia and filopodia surrounding the conidia. Membrane extensions next to conidia usually did not follow the shape of the conidium (Fig. 1C), while close continuous contact between the filopodia and the entire conidial surface was not detected. Contacts between filopodia and conidia were made at distinct and separate points (Fig. 1B, C, and G). Finally, the pseudopod extensions coalesced to engulf the conidium (Fig. 1D).

AMs were heterogeneous in shape and size but were gener-

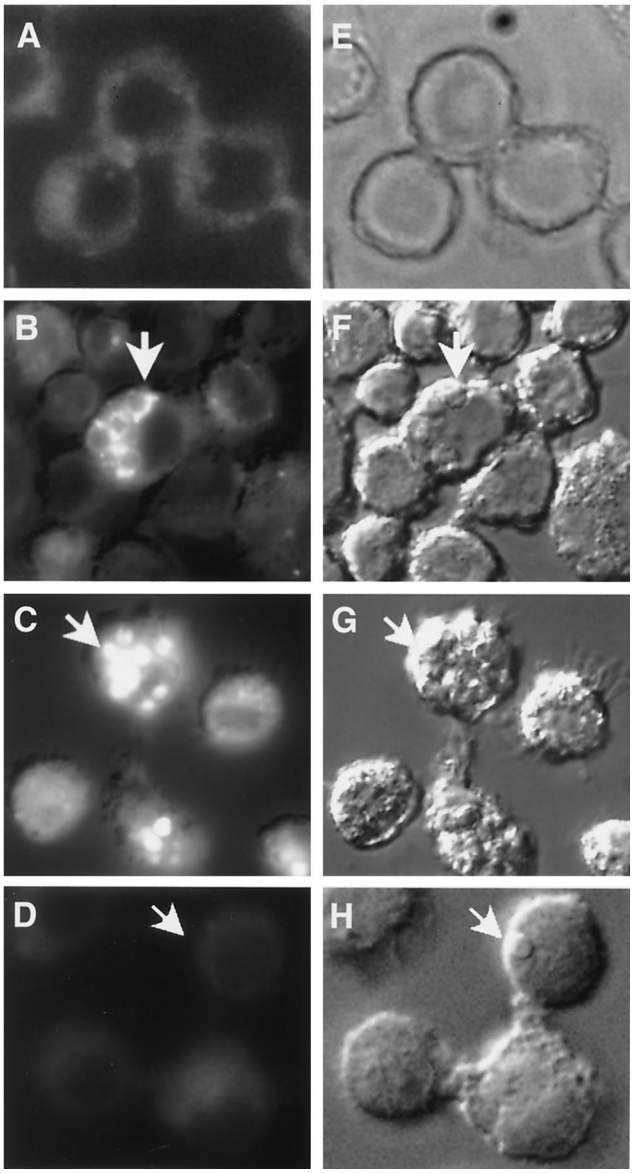

FIG. 6. Acidification of conidia-containing phagolysosomes. HAMs were incubated with the acidotropic probe LysoTracker Red DND-99 for 2 h, washed with RPMI complete medium, and incubated with conidia in RPMI complete medium containing LysoTracker. Control experiments were done in the presence of 250 nM bafilomycin A. (A) Negative control prior to conidial challenge. (B and C) At 4 h postinfection, the acidic pH in the phagolysosome was revealed by bright red fluorescence (arrows) surrounding the conidia (B) or impregnating the conidia (C). (D) Shown is a cell (arrow) with phagocytosed conidia incubated in the presence of bafilomycin A that is negative with LysoTracker. (E to H) Corresponding phase-contrast (E) and DIC (F to H) images. Bar, 2 μm.

ally round in shape with mean diameters (± standard error of the mean) of 13 ± 3 μm for HAMs and 10 ± 1.5 μm for MH-S cells. Phalloidin staining revealed that the majority of uninfected cells had many actin-filled filopodia or broad lamellipodia (Fig. 2a and b).

Actin polymerization and PI 3-kinase activity are required for *A. fumigatus* phagocytosis. During the first minutes following contact between AMs and conidia, Texas Red-phalloidin revealed that pseudopods surrounding the conidia were stained for F-actin. Phagocytic cups characterized by a local concentration of F-actin were detected at sites where conidia were attached (Fig. 2c and e). After engulfment, the F-actin-rich filopodia completely encircled the conidium (Fig. 2d and f).

Follow-up of F-actin staining in HAMs and MH-S cells during ingestion of *A. fumigatus* conidia showed that a maximal number (about 15% of the total number of conidia associated to macrophages) was capped with F-actin between 10 and 60 min from the beginning of phagocytosis in HAMs (Fig. 2g) and F-actin rings were observed to surround ingested conidia (Fig. 2d). At 3 h postinfection, phalloidin staining could no longer be detected around conidia. In contrast, in MH-S macrophages, only 5% of the conidia associated to macrophages were found to be capped with F-actin and this dropped to 0% 60 min after the beginning of ingestion (Fig. 2g). This could be due to a faster uptake of conidia by MH-S cells than by HAMs so that the rapid transient actin polymerization in phagocytic cups could not be detected within the time frame used in our experiments.

To confirm the role of actin in the phagocytic uptake of conidia by HAMs and MH-S cells, we investigated the effect of cytochalasin D, a drug that inhibits polymerization of actin in the process of conidia internalization. Incubation of infected MH-S cells with 2 μM cytochalasin D blocked the uptake of conidia, and 7% ± 2% of conidia were internalized by cytochalasin D-treated MH-S cells. Cytochalasin D had a similar inhibitory effect on the phagocytosis of conidia by HAMs (data not shown). As expected, treatment with cytochalasin D resulted in significant changes in cellular morphology, as shown by scanning electron microscopy (Fig. 3). The entire cell morphology was altered, and blebs and balloons, most probably nuclei, were observed to be bulging from the top of the cells (Fig. 3A). In drug-treated cells, phalloidin staining revealed discontinuous cortical actin and aggregates of actin were brightly stained at the cell periphery (Fig. 3B). Although conidia were still bound to AMs, they remained extracellular (Fig. 3C).

The effect of wortmannin, a drug that inhibits PI 3-kinase, was also investigated in order to further study the molecular events contributing to *A. fumigatus* phagocytosis. PI 3-kinase is known to be involved in Fc gamma receptor (FcγR)- and complement receptor-3 (CR3)-dependent phagocytic uptake. As was observed with cytochalasin D, wortmannin also blocked conidia uptake by both HAMs and MH-S cells, and 11% ± 2% of conidia were internalized by wortmannin-treated MH-S cells. The cell morphology was also altered following incubation with 1 μM wortmannin. Scanning electron microscopy as well as phalloidin staining of the wortmannin-treated cells showed that cells had smooth surfaces with short filopodia, and only cortical actin could be detected with phalloidin staining (Fig. 3D to E). These results showed that phagocytosis of conidia by AMs was entirely dependent on actin polymerization and on PI 3-kinase activity.

Intracellular fate of *A. fumigatus* conidia in AMs. Once internalized, an *A. fumigatus* conidium is contained within a phagosome surrounded by a well-defined phagosomal membrane that is tightly associated with the conidium surface (transmission electron microscopy data not shown).

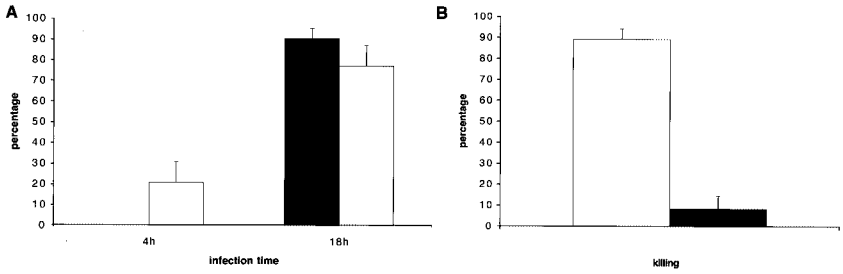

FIG. 7. Estimation of the capacity of MH-S cells to kill *A. fumigatus* conidia. (A) Killing of conidia (estimated as the percentage of nongerminating conidia) (solid column) and phagosomal acidification (estimated as the percentage of *A. fumigatus*-containing phagosomes positive for LysoTracker labeling) (open columns) at 4 and 18 h following ingestion. Values represent means plus standard deviations from three experiments. (B) Effect of bafilomycin A on the capacity of MH-S cells to kill *A. fumigatus* conidia. Untreated control cells (open column) and cells treated with 250 nM bafilomycin A (solid column) were allowed to ingest conidia, and the percentages of killing following 18 h of ingestion are shown.

We used antibodies specifically recognizing various membrane markers of the endocytic pathway such as TfR, EEA1, Rab7, and the lysosomal membrane protein (Lamp1) to determine the extent to which the *A. fumigatus*-containing phagosomes interacted with compartments of the endocytic pathway. Since these proteins are markers of early events in the formation and maturation of the phagolysosome, observations were carried out for only 1 h after the beginning of infection.

In HAMs, a positive signal by immunofluorescence was detected around ingested conidia with antibodies directed against TfR, EEA1, Rab7, and Lamp1. In all cases, the presence of a fluorescent halo surrounding the conidia was considered a positive signal (Fig. 4a to d). Control antibodies did not label any phagosome-like structure (see Fig. 4l for an example). In addition, the specificity of the immunolabeling was confirmed by the fact that conidia attached to the outer membrane of the cell were negative with all of the above-mentioned antibodies (Fig. 4c and j).

The kinetics of appearance of the specific immunolabeling for TfR, EEA1, Rab7, and Lamp1 in the conidia-containing phagosomes in infected HAMs is shown in Fig. 5A. The highest percentage of positive phagosomes containing conidia (i.e., [the number of antibody-labeled phagosomes containing conidia/total number of phagosomes containing conidia] $\times$ 100) was seen 10 to 30 min after the beginning of conidia internalization. The number of positive phagosomes was highly reduced after 1 h of phagocytosis. In contrast, the number of anti-Lamp1-positive phagosomes increased during the course of ingestion and was identical to the number of ingested conidia (Fig. 5A). All ingested conidia were found to have a Lamp1-positive ring around them, and they remained Lamp1 positive for up to 18 h postinfection.

The labeling pattern detected in the MH-S cells was identical to that observed in HAMs (data not shown). Figure 5B shows the kinetics of appearance of TfR, Rab7, and Lamp1 staining in the phagolysosome of MH-S cells. The maximal number of TfR- and Rab7-positive phagosomes was detected 5 min postinfection, which was earlier than in the HAMs. Labeling with the anti-Lamp1 antibody gave similar results for the MH-S cells and the HAMs.

Thus, following ingestion, phagosomes containing conidia of *A. fumigatus* acquired specific markers of the endocytic pathway membrane compartments. The kinetics of appearance of each of these markers in the phagosome also indicated that conidia-containing phagosomes mature into phagolysosomes.

Acidification of the phagolysosomes containing *A. fumigatus* conidia. The acidotropic probe LysoTracker Red DND-99 is a weak base conjugated to a red fluorophore that freely permeates cell membranes; upon protonation, it remains trapped in acidified organelles. This probe was used to investigate the pH changes in the phagolysosome after ingestion of the *A. fumigatus* conidia.

The acidic pH in the phagolysosome was revealed by red fluorescent labeling surrounding or totally covering the conidia inside the phagolysosome, appearing in the latter case as bright red spots (Fig. 6B and C). Uninfected HAMs did not show any fluorescence with LysoTracker (Fig. 6A). Uninfected and infected HAMs were incubated with bafilomycin A, an inhibitor of lysosomal vacuolar ATPase, thereby blocking the acidification of the late endocytic compartments and neutralizing the pH in the lysosomes (15). The inhibition of the lysosomal acidification was revealed by the absence of any fluorescence in the lysosomes of the bafilomycin A-treated cells (Fig. 6D). Similar labeling was detected in the bafilomycin A-treated or untreated MH-S cells (data not shown).

The percentage of conidia labeled in fluorescent red by the LysoTracker dye was comparable to the percentage of conidia killed by the macrophages (Fig. 7A). Four hours after ingestion, no killing of conidia could be detected and the percentage of acidic phagolysosomes was low (20% in MH-S cells and 12% in HAMs). In contrast, after 18 h of incubation, where a high level of conidia killing was found (59 and 91% for HAMs and MH-S cells, respectively), the percentage of conidia labeled with red fluorescence was also high (57 and 77% for HAMs and MH-S cells, respectively).

To confirm the importance of acidification in the phagolysosomes of macrophages for the killing of *A. fumigatus* conidia, infected cells were incubated with bafilomycin A. Incubation of the MH-S cells or HAMs (data not shown) with 100 or 250 nM bafilomycin A almost abolished the conidial killing by AMs even after infection for 18 h (Fig. 7B).

Positive labeling was detected around the conidia in the phagolysosome when HAMs infected with conidia were probed with the anti-cathepsin D antibody. Positive labeling was observed very early after phagocytosis (as early as 5 min postinternalization in some cells) (Fig. 8A). A double immu-

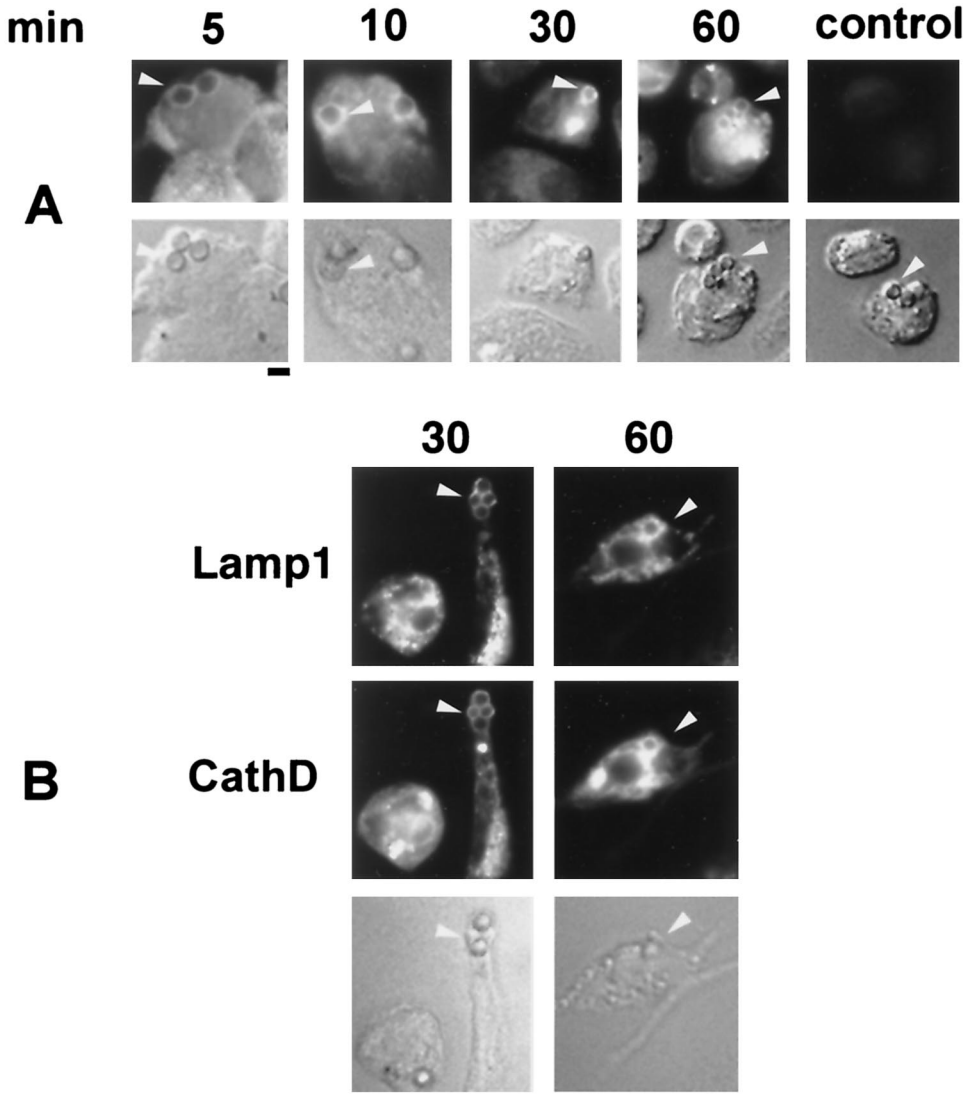

FIG. 8. Kinetics of cathepsin D acquisition by the conidia-containing phagosome. Phagocytosis of *A. fumigatus* by HAMs was initiated at 37°C after 30 min of incubation at 4°C with conidia at a 2:1 ratio of conidia to macrophages. (A) After different incubation times (5 to 60 min), cells were fixed, permeabilized, and stained with a pAb specific for cathepsin D and a secondary antibody conjugated with Texas Red (upper panels). Arrowheads indicate positive staining surrounding the conidia. Corresponding DIC images are also shown (lower panels). For the control, purified rabbit IgG was used instead of the anti-cathepsin D pAb. Bar, 2 μm. (B) Colocalization of Lamp1 and cathepsin D (arrowheads) at 30 and 60 min postinfection. Cells were labeled with the anti-Lamp1 MAb followed by the anti-cathepsin D pAb and successive labeling with FITC- and Texas Red-conjugated corresponding secondary antibodies. Arrowheads indicate staining surrounding conidia.

nofluorescence assay showed that Lamp1 and cathepsin D colocalized in the conidia-containing phagolysosome (Fig. 8B).

DISCUSSION

Macrophages play a key role in host defense against virtually all pathogenic microorganisms. Within macrophages, phagosomal maturation is a fundamental biological process for the control of intracellular pathogens (54). But is the maturation of a phagosome containing a fungal pathogen that leads to fungal killing different from that of a phagosome containing a fungal pathogen that does not lead to fungal killing?

In spite of the large number of in vitro studies on the involvement of different host products such as oxygen radicals, hydrolases, cationic proteins, and defensins in the defense against fungal infection (25), only a few studies have investigated the maturation of phagosomes containing fungal pathogens.

A. fumigatus provides a useful experimental model for exploring cellular mechanisms in AMs involved in phagocytosis, endocytic organelle movement, and organelle fusions. This study represents the first detailed description of the intracellular trafficking and fate of *A. fumigatus* in AMs.

First, phagocytosis of *A. fumigatus* conidia by AMs depends on local actin polymerization at the site of contact between the conidia and the macrophage. Actin reorganization has been repeatedly reported as one of the first molecular events in-

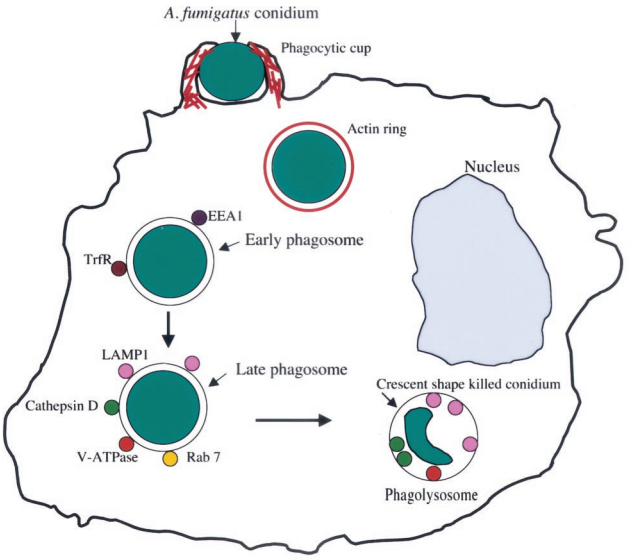

FIG. 9. Model of phagocytosis of *A. fumigatus* by AMs. V-ATPase, vacuolar ATPase.

volved in the phagocytic internalization of most microorganisms (35, 69). Entry of *A. fumigatus* conidia into AMs is morphologically similar to the trigger mechanism (29) used by bacteria like *Salmonella* or *Shigella* species (1, 4, 31, 54). Similar morphological engulfment and actin reorganization have also been described during phagocytosis of the pathogenic yeast *Candida albicans* by peritoneal macrophages (44), as well as in epithelial cells (70). However, in contrast to what is known about bacterial entry into mammalian cells, no *A. fumigatus* conidial protein has yet been shown to be active in macrophage surface membrane remodeling.

Numerous studies have shown that F-actin polymerization is a short-lived and transient event. Condensation of F-actin usually disappears from the periphery of the phagosome after the microorganisms have been fully internalized (2, 37). This leaves the phagosome membrane available to fuse with endosomes and lysosomes (3, 10). This idea has recently been challenged by data showing that actin assembly is required for phagosome-endosome fusion (26), while other studies (reviewed by May and Machesky [50]), have suggested that the phagosome membrane retains for a long time proteins that facilitate interaction with the actin cytoskeleton.

In agreement with the latter hypothesis, our data showed continuous enrichment of actin on *A. fumigatus*-containing phagosomes. F-actin rings surrounding the phagosomes containing conidia in HAMs could be detected even at 1 h postinfection. In contrast to our results, Kaposzta et al. (44) found in their study of *C. albicans* phagocytosis that condensation of actin filaments around phagosomes of mouse peritoneal macrophages infected with *C. albicans* could be observed only during the first 5 min of yeast internalization.

The role of F-actin during phagocytosis was confirmed by the complete inhibition of conidial uptake by cytochalasin D. Cytochalasin D (22) causes the depolymerization of actin microfilaments (30), and it has been repeatedly reported that disruption of filamentous actin blocks yeast phagocytosis (14, 44). Wortmannin also blocked conidial uptake. It is known that wortmannin irreversibly inhibits the PI 3-kinases required for FcγR- and CR3-mediated phagocytosis (8, 23, 24). PI 3-kinases have been reported to provide material for membrane extension around the particle and to control closure of the phagosome rather than to regulate the initial actin polymerization during phagocytosis (8, 24). Inhibition of PI 3-kinases thereby prevents the completion of phagocytosis. Such a mechanism could be responsible for the inhibition by wortmannin of *A. fumigatus* phagocytosis.

Maturation of the *A. fumigatus*-containing phagosomes was monitored by immunofluorescence microscopy using a panel of antibodies recognizing endogenous markers of the endocytic pathway. Both early endosomes containing the TfR and EEA1 markers and late endosomes containing Rab7 fused with phagosomes 5 to 30 min postinternalization. EEA1 is a membrane-associated protein localized to the early endosomes (57) and has been shown to be a tethering protein implicated in the docking of incoming endocytic vesicles, thereby providing directionality to early-endosome fusion (75). Moreover, it has been demonstrated that EEA1 can play roles in the acquisition by phagosomes of molecules from the biosynthetic pathway (34) and in phagosomal maturation (32).

The TfR is a specific marker of the early endosomes (18, 39, 41, 51). The extensive network of TfR-positive tubules and vesicles in membrane recycling has been demonstrated in macrophages. This recycling process has been shown to promote phagocytosis of erythrocytes by macrophages (23). The TfR has also been detected on *Salmonella*-containing vacuoles (41) in macrophages as well as in *Toxoplasma gondii*-containing phagosomes (56).

In addition to the early endosomal markers, the *A. fumigatus*-containing phagosomes also acquired the late endocytic marker Rab7. Rab7 is a small GTPase playing a central role in the transport steps connecting late endosomes to upstream and downstream endocytic compartments and possibly to the phagocytic route (53, 60).

The acquisition of lysosomal characteristics by *A. fumigatus* phagosomes was monitored with antibodies specific for the Lamp1 or cathepsin D proteins, two markers of the late stages of phagolysosome development (17, 65, 66). The maturation of the *A. fumigatus*-containing phagosomes into a lysosome-like compartment was observed within the first 5 min of phagocytosis. Lamp1 and cathepsin D were found on the phagolysosomes at the first time point examined and accumulated over the entire length of the infection. Similar results demonstrating a rapid fusion between phagosomes and lysosomes during the phagocytosis of *Candida albicans* (44), *Salmonella enterica* serovar Typhimurium, and *Yersinia pseudotuberculosis* (55, 56, 61) by macrophages have been reported. Lamp1 was detected in phagosomes containing *A. fumigatus* until the conidia were killed by the macrophage.

The capacity of the macrophage to efficiently degrade the phagocytosed microorganisms has been shown repeatedly (20, 21, 76). Vacuolar ATPases involved in the acidification of the phagosome accumulate in the phagosomal membrane during maturation (40, 71).

Acidification of the phagosome, associated with the activation of lysosomal hydrolytic enzymes, is a critical step in the degradation event (28, 38, 73). Accordingly, *A. fumigatus*-con-

taining phagosomes contained the lysosomal hydrolase cathepsin D. This suggested that lysosomal hydrolases could be involved in the degradation of *A. fumigatus* conidia. Other lytic enzymes such as chitinase that can play a role in the degradation of conidial cell walls containing chitin have also been shown to be present in macrophages (13). Their role in the killing of *A. fumigatus* conidia has not yet been investigated.

The lysosomal acidification of *A. fumigatus* phagosomes was monitored with a fixable acidotropic fluorescent probe, LysoTracker Red DND-99, which has been used previously to monitor maturation of the phagosome within macrophages infected by *Mycobacterium tuberculosis* (72) and to stain acidic organelles in neuronal cells (74). When lysosomal acidification was blocked by incubation of the AMs with bafilomycin A (15), which specifically blocks the vacuolar proton ATPase in the endosomal membrane (19), the killing of *A. fumigatus* conidia was dramatically reduced. This finding was consistent with previous observations. Bafilomycin A significantly depressed the intracellular killing of *Staphylococcus aureus* (12) as well as the amebic lysis of epithelial cells (33). Moreover, we found in our study that the effect of bafilomycin A was not restricted only to an inhibition of the lysosome acidification, since this drug caused detectable changes in AM morphology, particularly a shortening of cell filopodia. This was associated with a 30% reduction of *A. fumigatus* uptake by AMs in the presence of 250 nM bafilomycin A. At this concentration, the viability of the macrophages was not altered (data not shown). Similar effects have been reported in a study of bacterial and erythrocyte uptake by *Entamoeba histolytica* (12, 33).

Suppression of conidia killing upon vacuolar ATPase inhibition could be due to the increase in intralysosomal pH, but it might also be due to a reduction in superoxide production (58, 68). Reactive oxidants have recently been shown to play an essential role in *A. fumigatus* killing by AMs (B. Philippe, O. Ibrahim-Granet, M. C. Prévost, M. A. Gougerot-Pocidalo, M. Sanchez Perez, A. Van der Meerew, and J. P. Latgé, submitted for publication).

Based on the data acquired to date, using both a murine cell line and primary cells obtained from human lung lavages, the following model for the phagocytosis of *A. fumigatus* conidia by AMs can be established (Fig. 9). (i) An *A. fumigatus* conidium is bound to an AM by an as-yet-unidentified receptor(s) and mechanisms. (ii) This triggers the formation of actin-dependent membrane protrusions or pseudopodia around the conidium. (iii) Actin-dependent enhancement of the phagocytic cup and fusion of the pseudopodia lead to particle internalization. (iv) Phagosomes are fusogenic with endosomal compartments and thereby acquire and lose early and late endosome markers. (v) Final maturation of the *A. fumigatus* phagosome is associated with the acquisition and maintenance of Lamp1 and acidification of the phagolysosome. This phagocytic scheme is similar to the generally accepted model which holds that phagosomes successively display markers of early and late endosomes and lysosomes (27, 56, 61).

The role of pH in intracellular trafficking in the macrophage depends on the species of the fungal pathogen. In contrast to what occurs with *A. fumigatus*, the acidic pH of the phagolysosome favors the survival and germ tube formation of *C. albicans* in the phagolysosome, leading to the destruction of the macrophage (44). The strategy for survival inside the macrophage used by *Histoplasma capsulatum* involves controlling the pH of its intraphagosomal environment at 6 to 6.5 by inhibition of phagolysosomal fusion and recruitment of the host vacuolar ATPase (59). The ability of *Cryptococcus neoformans* to survive inside macrophages is also associated with the acidification of the phagolysosome. Drugs or nutrients that alkalinize the pH of the phagolysosome have been found to increase the activity of monocytes against *C. neoformans* (47). Uptake and degradation of *Pneumocystis carinii* by alveolar macrophages has been reported, but the trafficking of this fungus has not yet been investigated (48).

The exact contributions of the acidification of the phagolysosome, iron deprivation, and the activation of lysosomal enzymes to fungal killing or survival remain unknown for all fungi. The interactions of proton ions with reactive oxidant intermediates also merit investigation.

ACKNOWLEDGMENTS

We are very grateful to Alice Dautry (Unité de Biologie des Interactions Cellulaires, Institut Pasteur) for her advice as well as for providing the microscopy facilities for this study and to S. Méresse (Centre d'Immunologie de Marseille Luminy) for his helpful suggestions. We thank David Montero (Centre Interuniversitaire de Microscopie Electronique) for his technical assistance in the scanning electron microscopy.

This work was supported by a grant from le Ministère de l'Education Nationale, de la Recherche et de la Technologie.

REFERENCES

1. **Adam, T., M. Arpin, M. C. Prévost, P. Gounon, and P. J. Sansonetti.** 1995. Cytoskeletal rearrangements and the functional role of T-plastin during entry of *Shigella flexneri* into HeLa cells. J. Cell Biol. **129:**367–381.
2. **Aderem, A. A., and D. M. Underhill.** 1999. Mechanisms of phagocytosis in macrophages. Annu. Rev. Immunol. **17:**593–623.
3. **Allen, L. A. H., and A. A. Aderem.** 1995. A role for MARCKS, the α isozyme of protein kinase C and myosin I in zymosan phagocytosis by macrophages. J. Exp. Med. **182:**829–840.
4. **Alpuche-Aranda, C., E. L. Racoosin, J. A. Swanson, and S. I. Miller.** 1994. *Salmonella* stimulate macrophage macropinocytosis and persist within spacious phagosomes. J. Exp. Med. **179:**601–608.
5. **Alvarez-Dominguez, C., A. M. Barbieri, W. Beron, A. Wandinger-Ness, and P. D. Stahl.** 1996. Phagocytosed live *Listeria monocytogenes* influences Rab5-regulated *in vitro* phagosome-endosome fusion. J. Biol. Chem. **271:**13834–13843.
6. **Alvarez-Dominguez, C., R. Roberts, and P. D. Stahl.** 1997. Internalized *Listeria monocytogenes* modulates intracellular trafficking and delays maturation of the phagosome. J. Cell Sci. **110:**731–743.
7. **Alvarez-Dominguez, C., and P. D. Stahl.** 1999. Increased expression of Rab5a correlates directly with accelerated maturation of *Listeria monocytogenes* phagosomes. J. Biol. Chem. **274:**11459–11462.
8. **Araki, N., M. T. Johnson, and J. A. Swanson.** 1996. A role for phosphoinositide 3-kinase in the completion of macropinocytosis and phagocytosis by macrophages. J. Cell Biol. **135:**1249–1260.
9. **Arcaro, A., and M. P. Wymann.** 1993. Wortmannin is a potent phosphatidylinositol 3-kinase inhibitor: the role of phosphatidylinositol 3,4,5-trisphosphate in neutrophil responses. Biochem. J. **296:**297–301.
10. **Bengtsson, T., M. E. E. Jaconi, M. Gustafson, K. E. Magnusson, J. M. Theler, D. P. Lew, and O. Standahl.** 1993. Actin dynamics in human neutrophils during adhesion and phagocytosis is controlled by changes in intracellular free calcium. Eur. J. Cell Biol. **62:**49–58.
11. **Beron, W., C. Alvarez-Dominguez, L. Mayorga, and P. D. Stahl.** 1995. Membrane trafficking along the phagocytic pathway. Trends Cell Biol. **5:**100–104.
12. **Bidani, A., B. S. Reisner, A. K. Haque, J. Wen, R. E. Helmer, D. M. Tuazon, and T. A. Hemoing.** 2000. Bactericidal activity of alveolar macrophages is suppressed by V-ATPase inhibition. Lung **178:**91–104.
13. **Boot, R. G., G. H. Renkema, A. Strijland, A. J. van Zonneveld, and J. M. Aerts.** 1995. Cloning of a cDNA encoding chitotriosidase, a human chitinase produced by macrophages. J. Biol. Chem. **270:**26252–26256.
14. **Bos, H., and W. de Souza.** 2000. Phagocytosis of yeast: a method for concurrent quantification of binding and internalization using differential interference contrast microscopy. J. Immunol. Methods **238:**29–43.
15. **Bowman, E. J., A. Siebers, and K. Altendorf.** 1988. Bafilomycins: a class of inhibitors of membrane ATPases from microorganisms, animal cells, and plant cells. Proc. Natl. Acad. Sci. USA **85:**7972–7976.

16. **Charpin, J. M., M. Stern, D. Grenet, and D. Israël-Biet.** 2000. Insulinlike growth factor-1 in lung transplants with obliterative bronchiolitis. Am. J. Respir. Crit. Care Med. **161:**1991–1998.
17. **Chen, J. W., Y. Cha, K. U. Yuksel, R. W. Gracy, and J. T. August.** 1988. Isolation and sequencing of a cDNA clone encoding lysosomal membrane glycoprotein mouse LAMP-1. Sequence similarity to proteins bearing oncodifferentiation antigens. J. Biol. Chem. **263:**8754–8758.
18. **Ciechanover, A., A. L. Schwartz, A. Dautry-Varsat, and H. F. Lodish.** 1983. Kinetics of internalization and recycling of transferrin and the transferrin receptors in a human hepatoma cell line. J. Biol. Chem. **9:**9681–9689.
19. **Clague, M. J.** 1999. Membrane transport: take your fusion partners. Curr. Biol. **9:**R258–R260.
20. **Claus, V., A. Jahraus, T. Tjelle, T. Berg, H. Kirschke, H. Faulstich, and G. Griffiths.** 1998. Lysosomal enzyme trafficking between phagosomes, endosomes, and lysosomes in J774 macrophages. J. Biol. Chem. **273:**9842–9851.
21. **Clemens, D. L., B. Y. Lee, and M. A. Horwitz.** 2000. Deviant expression of Rab5 on phagosomes containing the intracellular pathogens *Mycobacterium tuberculosis* and *Legionella pneumophila* is associated with altered phagosomal fate. Infect. Immun. **68:**2671–2684.
22. **Cooper, J. A.** 1987. Effects of cytochalasin and phalloidin on actin. J. Cell Biol. **105:**1473–1478.
23. **Cox, D., D. J. Lee, B. M. Dale, J. Calafat, and S. Greenberg.** 2000. A Rab11-containing rapidly recycling compartment in macrophages that promotes phagocytosis. Proc. Natl. Acad. Sci. USA **97:**680–685.
24. **Cox, D., C. C. Tseng, G. Bjekic, and S. Greenberg.** 1999. A requirement for phosphatidylinositol 3-kinase in pseudopod extension. J. Biol. Chem. **274:** 1240–1247.
25. **Cox, R. A.** 1989. Immunology of the fungal diseases. CRC Press, Inc., Boca Raton, Fla.
26. **Defacque, H., M. Egeberg, A. Habermann, M. Diakonova, C. Roy, P. Mangeat, W. Voelter, G. Marriott, J. Pfannstiel, H. Faulstich, and G. Griffiths.** 2000. Involvement of ezrin/moesin in *de novo* actin assembly on phagosomal membranes. EMBO J. **19:**199–212.
27. **Desjardins, M., L. A. Huber, R. G. Parton, and G. Griffiths.** 1994. Biogenesis of phagolysosomes proceeds through a sequential series of interactions with the endocytic apparatus. J. Cell Biol. **124:**677–688.
28. **Downey, G. P., R. J. Botelho, J. R. Butler, Y. Moltyaner, P. Chien, A. D. Schreiber, and S. Grinstein.** 1999. Phagosomal maturation, acidification, and inhibition of bacterial growth in nonphagocytic cells transfected with FcγRIIA receptors. J. Biol. Chem. **274:**28436–28444.
29. **Dramsi, S., and P. Cossart.** 1998. Intracellular pathogens and the actin cytoskeleton. Annu. Rev. Cell Dev. Biol. **14:**137–166.
30. **Finlay, B. B., and S. Falkow.** 1997. Common themes in microbial pathogenicity revisited. Microbiol. Mol. Biol. Rev. **61:**136–169.
31. **Francis, C. L., M. N. Starnbach, and S. Falkow.** 1992. Morphological and cytoskeletal changes in epithelial cells occur immediately upon interaction with *Salmonella typhimurium* grown under low-oxygen conditions. Mol. Microbiol. **6:**3077–3087.
32. **Fratti, R. A., J. M. Backer, J. Gruenberg, S. Corvera, and D. Deretic.** 2001. Role of phosphatidylinositol 3-kinase and Rab5 effectors in phagosomal biogenesis and mycobacterial phagosome maturation arrest. J. Cell Biol. **154:**631–644.
33. **Ghosh, S. K., and J. Samuelson.** 1997. Involvement of $p21^{racA}$, phosphoinositide 3-kinase, and vacuolar ATPase in phagocytosis of bacteria and erythrocytes by *Entamoeba histolytica*: suggestive evidence for coincidental evolution of amebic invasiveness. Infect. Immun. **65:**4243–4249.
34. **Gillooly, D. J., A. Simonsen, and H. StenMark.** 2001. Phosphoinositides and phagocytosis. J. Cell Biol. **155:**15–17.
35. **Greenberg, S.** 1999. Modular components of phagocytosis. J. Leukoc. Biol. **66:**712–717.
36. **Greenberg, S., K. Burridge, and S. C. Silverstein.** 1990. Colocalization of F-actin and talin during Fc receptor-mediated phagocytosis in mouse macrophages. J. Exp. Med. **172:**1853–1856.
37. **Greenberg, S., J. El Khoury, F. Di Virgilio, E. M. Kaplan, and S. C. Silverstein.** 1991. Ca^{2+}-independent F-actin assembly and disassembly during Fc receptor-mediated phagocytosis in mouse macrophages. J. Cell Biol. **113:** 757–767.
38. **Grinstein, S., A. Nanda, G. Lukacs, and O. Rotstein.** 1992. V-ATPases in phagocytic cells. J. Exp. Biol. **172:**179–192.
39. **Gruenberg, J., and F. R. Maxfield.** 1995. Membrane transport in the endocytic pathway. Curr. Opin. Cell Biol. **7:**552–563.
40. **Hackam, D. J., O. D. Rotstein, W. J. Zhang, N. Demaurex, M. Woodside, O. Tsai, and S. Grinstein.** 1997. Regulation of phagosomal acidification. J. Biol. Chem. **272:**29810–29820.
41. **Hashim, S., K. Mukherjee, M. Raje, S. K. Basu, and A. Mukhopadhyay.** 2000. Live *Salmonella* modulate expression of Rab proteins to persist in a specialized compartment and escape transport to lysosomes. J. Biol. Chem. **275:**16281–16288.
42. **Howard, T. H., and R. G. Watts.** 1994. Actin polymerization and leukocyte function. Curr. Opin. Hematol. **1:**61–68.
43. **Johnson, M. T., and S. Kornfelf.** 1992. A His-Leu-Leu sequence near the carboxyl terminus of the cytoplasmic domain of the cation-dependent mannose 6-phosphate receptor is necessary for the lysosomal enzyme sorting function. J. Biol. Chem. **267:**17110–17115.
44. **Kaposzta, R., L. Marodi, M. Hollinshead, S. Gordon, and R. P. da Silva.** 1999. Rapid recruitment of late endosomes and lysosomes in mouse macrophages ingesting *Candida albicans*. J. Cell Sci. **112:**3237–3248.
45. **Kornfelf, S., and I. Mellman.** 1989. The biogenesis of lysosomes. Annu. Rev. Cell Biol. **5:**483–525.
46. **Latgé, J.** 1999. *Aspergillus fumigatus* and aspergillosis. Clin. Microbiol. Rev. **12:**310–350.
47. **Levitz, S. M., S. H. Nong, K. F. Seetoo, T. S. Harrison, R. A. Speizer, and E. R. Simons.** 1999. *Cryptococcus neoformans* resides in an acidic phagolysosome of human macrophages. Infect. Immun. **67:**885–890.
48. **Limper, A. H., J. S. Hoyte, and J. E. Standing.** 1997. The role of alveolar macrophages in *Pneumocystis carinii* degradation and clearance from the lung. J. Clin. Investig. **99:**2110–2117.
49. **Matsunaga, K., T. W. Klein, H. Friedman, and Y. Yamamoto.** 2001. Alveolar macrophage cell line MH-S is valuable as an *in vitro* model for *Legionella pneumophila* infection. Am. J. Respir. Cell Mol. Biol. **24:**326–331.
50. **May, R. C., and L. M. Machesky.** 2001. Phagocytosis and the actin cytoskeleton. J. Cell Sci. **114:**1061–1077.
51. **Mayor, S., J. F. Presley, and F. R. Maxfield.** 1993. Sorting of membrane components from endosomes and subsequent recycling to the cell surface occurs by a bulk flow process. **12:**1257–1269.
52. **Méresse, S., J. P. Gorvel, and P. Chavrier.** 1995. The rab7 GTPase resides on a vesicular compartment connected to lysosomes. J. Cell Sci. **108:**3349–3358.
53. **Méresse, S., O. Steele-Mortimer, B. B. Finlay, and J. P. Gorvel.** 1999. The rab7 GTPase controls the maturation of *Salmonella typhimurium*-containing vacuoles in HeLa cells. EMBO J. **18:**4394–4403.
54. **Méresse, S., O. Steele-Mortimer, E. Moreno, M. Desjardins, B. Finlay, and J. P. Gorvel.** 1999. Controlling the maturation of pathogen-containing vacuoles: a matter of life and death. Nat. Cell Biol. **1:**E183–E188.
55. **Mills, S. D., and B. B. Finlay.** 1998. Isolation and characterization of *Salmonella typhimurium* and *Yersinia pseudotuberculosis*-containing phagosomes from infected mouse macrophages: *Y. pseudotuberculosis* traffics to terminal lysosomes where they are degraded. Eur. J. Cell Biol. **77:**35–47.
56. **Mordue, D. G., and L. D. Sibley.** 1997. Intracellular fate of vacuoles containing *Toxoplasma gondii* is determined at the time of formation and depends on the mechanism of entry. J. Immunol. **159:**4452–4459.
57. **Mu, F. T., J. M. Callaghan, O. Steele-Mortimer, H. StenMark, R. G. Parton, P. L. Campbell, J. McCluskey, J. P. Yeo, E. P. C. Tock, and B. H. Toh.** 1995. EEA1, an early endosome-associated protein. J. Biol. Chem. **270:**13503–13511.
58. **Murphy, C., and H. J. Forman.** 1993. Effects of sodium and proton pump activity on respiratory burst and pH regulation of rat alveolar macrophages. Am. J. Physiol. **264:**L523–L532.
59. **Newman, S. L.** 1999. Macrophages in host defense against *Histoplasma capsulatum*. Trends Microbiol. **7:**67–71.
60. **Novick, P., and M. Zerial.** 1997. The diversity of Rab proteins in vesicle transport. Curr. Opin. Cell Biol. **9:**496–504.
61. **Oh, Y. K., C. Alpuche-Aranda, E. Berthiaume, T. Jinks, S. I. Miller, and J. A. Swanson.** 1996. Rapid and complete fusion of macrophage lysosomes with phagosomes containing *Salmonella typhimurium*. Infect. Immun. **64:**3877–3883.
62. **Osborn, M., and K. Weber.** 1982. Immunofluorescence and immunocytochemical procedures with affinity purified antibodies: tubulin-containing structures. Methods Cell Biol. **24:**97–132.
63. **Pizarro-Cerda, J., S. Méresse, R. G. Parton, G. van der Goot, A. Sola-Landa, I. Lopez-Goni, E. Moreno, and J. P. Gorvel.** 1998. *Brucella abortus* transits through the autophagic pathway and replicates in the endoplasmic reticulum of nonprofessional phagocytes. Infect. Immun. **66:**5711–5724.
64. **Rathman, M., M. D. Sjaastad, and S. Falkow.** 1996. Acidification of phagosomes containing *Salmonella typhimurium* in murine macrophages. Infect. Immun. **64:**2765–2773.
65. **Richo, G. R., and G. E. Conner.** 1994. Structural requirements of procathepsin D activation and maturation. J. Biol. Chem. **269:**14806–14812.
66. **Rijnboutt, S., W. Stoorvogel, H. J. Geuze, and G. J. Strous.** 1992. Identification of subcellular compartments involved in biosynthetic processing of cathepsin D. J. Biol. Chem. **267:**15665–15672.
67. **Sturtevant, J., and J. P. Latgé.** 1992. Interactions between the spore of *Aspergillus fumigatus* and human complement component C3. Infect. Immun. **60:**1913–1918.
68. **Swallow, C. J., S. Grinstein, R. A. Sudsbury, and O. D. Rotstein.** 1993. Relative roles of Na^+/H^+ exchange and vacuolar-type H^+ ATPases in regulating cytoplasmic pH and function in murine peritoneal macrophages. J. Cell. Physiol. **157:**453–460.
69. **Tjelle, T. E., T. Lovdal, and T. Berg.** 2000. Phagosome dynamics and function. Bioessays **22:**255–263.
70. **Tsarfaty, I., H. Sandovsky-Losica, L. Mittelman, I. Berdicevsky, and E. Segal.** 2000. Cellular actin is affected by interaction with *Candida albicans*. FEMS Microbiol. Lett. **189:**225–232.
71. **Tsukano, H., F. Kura, T. Inoue, T. Sato, H. Izumiya, T. Yasuda, and H.**

Watanabe. 1999. *Yersinia pseudotuberculosis* blocks the phagosomal acidification of B10. A mouse macrophages through the inhibition of vacuolar H^+-ATPase activity. Microb. Pathog. **27:**253–263.
72. **Via, L. E., R. A. Fratti, M. McFalone, E. Pagan-Ramos, D. Deretic, and V. Deretic.** 1998. Effects of cytokines on mycobacterial phagosome maturation. J. Cell Sci. **111:**897–905.
73. **Watanabe, H., K. Kagaya, T. Yamada, and Y. Fukazawa.** 1991. Mechanism for candidacidal activity in macrophages activated by recombinant gamma interferon. Infect. Immun. **59:**521–528.
74. **White, B. H., and L. K. Kaczmarek.** 1997. Identification of a vesicular pool of calcium channels in the bag cell neurons of *Aplysia californica.* J. Neurosci. **17:**1582–1595.
75. **Wilson, J. M., M. de Hoop, N. Zorzi, B. H. Toh, C. G. Dotti, and R. G. Parton.** 2000. EEA1, a tethering protein of the early sorting endosome, shows a polarized distribution in hippocampal neurons, epithelial cells, and fibroblasts. Mol. Biol. Cell **11:**2657–2671.
76. **Woods, J., Q. Lu, M. A. Ceddia, and T. Lowder.** 2000. Exercise-induced modulation of macrophage function. Immunol. Cell Biol. **78:**545–553.

Editor: T. R. Kozel